Received: 20 November 2020 | Revised: 17 May 2021 | Accepted: 8 June 2021

DOI: 10.1111/bph.15601

RESEARCH ARTICLE

Targeting sphingosine kinase-1 with the low MW inhibitor SKI-5C suppresses the development of endometriotic lesions in mice

Jeannette Rudzitis-Auth | Anika Christoffel | Michael D. Menger | Matthias W. Laschke

Institute for Clinical & Experimental Surgery, Saarland University, Homburg/Saar, Germany

Correspondence
Jeannette Rudzitis-Auth, Institute for Clinical & Experimental Surgery, Saarland University, D-66421, Homburg/Saar, Germany.
Email: jeannette.rudzitis-auth@uks.eu

Background and Purpose: Limited evidence suggests that the sphingosine-1-phosphate/sphingosine kinase 1 (S1P/SPHK1) signalling pathway is involved in the pathogenesis of endometriosis. Therefore, we analyzed in this study whether the inhibition of SPHK1 and, consequently, decreased levels of S1P affected the vascularization and growth of endometriotic lesions.

Experimental Approach: Endometriotic lesions were surgically induced in the peritoneal cavity and the dorsal skinfold chamber of female BALB/c mice. The animals received a daily dose of the SPHK1 inhibitor SKI-5C or vehicle (control). Analyses involved the determination of lesion growth, cyst formation, microvessel density and cell proliferation within peritoneal endometriotic lesions by means of high-resolution ultrasound imaging, caliper measurement, histology and immunohistochemistry. In the dorsal skinfold chamber model the development of newly formed microvascular networks and their microhemodynamic parameters within endometriotic lesions were investigated by means of intravital fluorescence microscopy.

Key Results: SKI-5C significantly inhibited the development and vascularization of peritoneal endometriotic lesions, as indicated by a reduced growth and cyst formation, a lower microvessel density and a suppressed cell proliferation, when compared to vehicle-treated controls. Endometriotic lesions in dorsal skinfold chambers of SKI-5C-treated animals exhibited a significantly smaller lesion size, lower functional microvessel density, smaller microvessel diameters and a reduced blood perfusion of the newly developing microvascular networks.

Conclusions and Implications: SPHK1/S1P signalling promotes the establishment and progression of endometriotic lesions. The inhibition of this pathway suppresses the development of endometriotic lesions, suggesting SPHK1 as a potential novel target for future endometriosis therapy.

Abbreviations: ERα, estrogen receptor-α; ERβ, estrogen receptor-β; FCS, Foetal calf serum; HIF-1α, hypoxia-inducible factor 1-α; S1P, sphingosine-1-phosphate; SKI-5C, 2,2-dimethyl-4S-(1-oxo-2-hexadecyn-1-yl)-1,1-dimethylethyl ester-3-oxazolidine carboxylic acid; SPHK1, sphingosine kinase-1; SPHK2, sphingosine kinase-2; StaR, steroidogenic acute regulatory protein.

KEYWORDS
angiogenesis, dorsal skinfold chamber, endometriosis, endometriotic lesions, high-resolution ultrasound imaging, proliferation, sphingosine kinase 1, vascularization

1 | INTRODUCTION

As a widespread and common disease, endometriosis affects about 5%–10% of women during their reproductive years. Typical symptoms are dysmenorrhea, chronic pelvic pain and infertility, which significantly impair the patients' quality of life (Soliman et al., 2016). Endometriosis is characterized by the occurrence of endometrial glands and stroma-like tissue outside the uterine cavity (Burney & Giudice, 2012). Although the disease has been known for a long time, its aetiology and pathogenesis still remain undefined. In 1927, Sampson proposed the widely spread theory that shed endometrium reaches the peritoneal cavity via retrograde menstruation, where it finally implants at ectopic sites (Sampson, 1927). The further development of the ectopic tissue is then crucially dependent on an adequate blood supply and, hence, the formation of new microvessels (Groothuis et al., 2005).

Different mechanisms are considered to contribute to the vascularization of endometriotic lesions, including angiogenesis, inosculation and vasculogenesis (Laschke & Menger, 2018). The formation of a new microvascular network is mainly driven by hypoxia and modulated by multiple pro- and anti-angiogenic factors (Rocha et al., 2013). Among them, the pro-angiogenic factor, **sphingosine-1-phosphate (S1P)**, a bioactive sphingolipid metabolite, is thought to play a major role in vascular development (Ader et al., 2009). S1P is generated by two isoforms of sphingosine kinase (**SPHK1** and **SPHK2**) through phosphorylation of the metabolic precursor **sphingosine** (Liu et al., 2002). The activation of SPHK1 is mediated by stimuli such as **VEGF**, which initiates endothelial cell sprouting (Ader et al., 2009). S1P is excreted into the extracellular space via specific transporters, such as spinster 2 (Nagahashi et al., 2013). Exogenous S1P is a ligand of five GPCRs, **$S1P_{1\text{-}5}$**, and regulates essential cellular processes, including angiogenesis, proliferation, migration, cytoskeletal organization, adherence junction assembly and morphogenesis (Sanchez & Hla, 2004). Intracellularly, S1P functions receptor-independently as second messenger, affecting calcium homeostasis, cell growth and apoptosis (Olivera et al., 2003).

Several studies reported a positive effect of the inhibition of SPHK and the reduction of cellular S1P levels in the treatment of tumours as well as inflammatory, hyperproliferative and vascular diseases (Datta et al., 2014; Mathews et al., 2010). In addition, decreasing S1P concentrations following the inhibition of SPHK1 have been shown to attenuate angiogenesis in different pathologies (Ader et al., 2015; Dai et al., 2017). Moreover, Santulli and co-workers demonstrated that the expression of S1P receptors and enzymes of the S1P pathway, such as SPHK1, are deregulated in the endometrium and endometriotic tissue of endometriosis patients (Santulli et al., 2012). Based on these findings, we analyzed in the present study whether the targeting of SPHK1 with the specific inhibitor SKI-5C affects the development and vascularization of endometriotic lesions in two different mouse models of the disease.

What is already known

- Vascularization is a hallmark of endometriosis.
- The sphingosine-1-phosphate signalling pathway is deregulated in endometriosis.

What does this study add

- The sphingosine kinase-1 inhibitor SKI-5C suppresses the development of endometriotic lesions.
- Inhibition of sphingosine kinase-1signalling reduces the formation of new microvascular networks.

What is the clinical significance

- Sphingosine kinase-1 represents a promising pharmacological target for the treatment of endometriosis.

2 | METHODS

2.1 | Animals

All animal care and experimental protocols were approved by the local governmental animal protection committee (Landesamt für Verbraucherschutz, Saarbrücken, Germany; permission number: 32/2015) and conducted according to the Directive 2010/63/EU. Animal studies are reported in compliance with the ARRIVE guidelines (Percie du Sert et al., 2020) and with the recommendations made by the *British Journal of Pharmacology* (Lilley et al., 2020).

As donor animals for the generation of uterine tissue grafts and as recipient animals for the induction of endometriotic lesions in the peritoneal cavity and in dorsal skinfold chambers, we used female BALB/c mice with an age of 12–16 weeks and a weight of 18–25 g (Institute for Clinical and Experimental Surgery, Saarland University, Homburg/Saar, Germany). The animals were housed in a conventional animal facility of the Institute for Clinical and Experimental Surgery, either 1 (dorsal skinfold chamber model) or 4–6 (peritoneal

endometriosis model) per cage, on wood chips as bedding. They were maintained under a 12-h day/night cycle and had free access to tap water and standard pellet food (Altromin, Lage, Germany).

2.2 | Vaginal lavage

In this study, we only included animals with normal oestrous cycles. The oestrous cycle was evaluated once daily by the cytological analysis of vaginal lavage samples, 1 week prior to the beginning of the experiments. In brief, 15 µl of 0.9% saline was carefully pipetted into the vagina. The resulting cell suspension was subsequently transferred to a glass slide and the cycle stage was determined under a phase contrast microscope (CH-2; Olympus, Hamburg, Germany). Only animals in the stage of oestrus were used as donor and recipient mice for the transplantation of uterine tissue samples into the peritoneal cavity to exclude differences between individual animals related to different sex hormone levels. For the implantation of the dorsal skinfold chamber, mice in the stage of dioestrus were used. After the implantation, they were allowed to recover for 48 h and, thus, to enter the oestrus stage. Thereafter, they also received endometrial fragments from donor mice in the stage of oestrus.

2.3 | Induction of endometriotic lesions

To investigate the effect of SPHK1 inhibition on the development of endometriotic lesions, a well-established mouse model of endometriosis was used (Rudzitis-Auth et al., 2020). For this purpose, two uterine tissue samples were sutured to the left and the right abdominal wall of recipient mice. BALB/c donor mice in the stage of oestrus were anaesthetized by an i.p. injection of 75 mg kg^{-1} ketamine and 15 mg kg^{-1} xylazine. After midline laparotomy, the uterine horns of the donor mice were isolated and placed into a petri dish containing DMEM (10% FCS, 100-U ml^{-1} penicillin, 0.1-mg ml^{-1} streptomycin). Subsequently, the uterine horns were openend longitudinally and 2-mm tissue samples were carefully removed by means of a dermal biopsy punch (Figure 1a), as previously described (Rudzitis-Auth et al., 2020).

For the surgical induction of endometriotic lesions, recipient mice were anaesthetized as described above and after midline laparotomy the uterine tissue samples were fixed with a 6-0 Prolene suture to the right and left lateral abdominal wall (Figure 1b,c). The laparotomy was then closed with running 6-0 Prolene muscle and skin sutures and the animals received a s.c. injection of 5-mg kg^{-1} carprofen as pain medication.

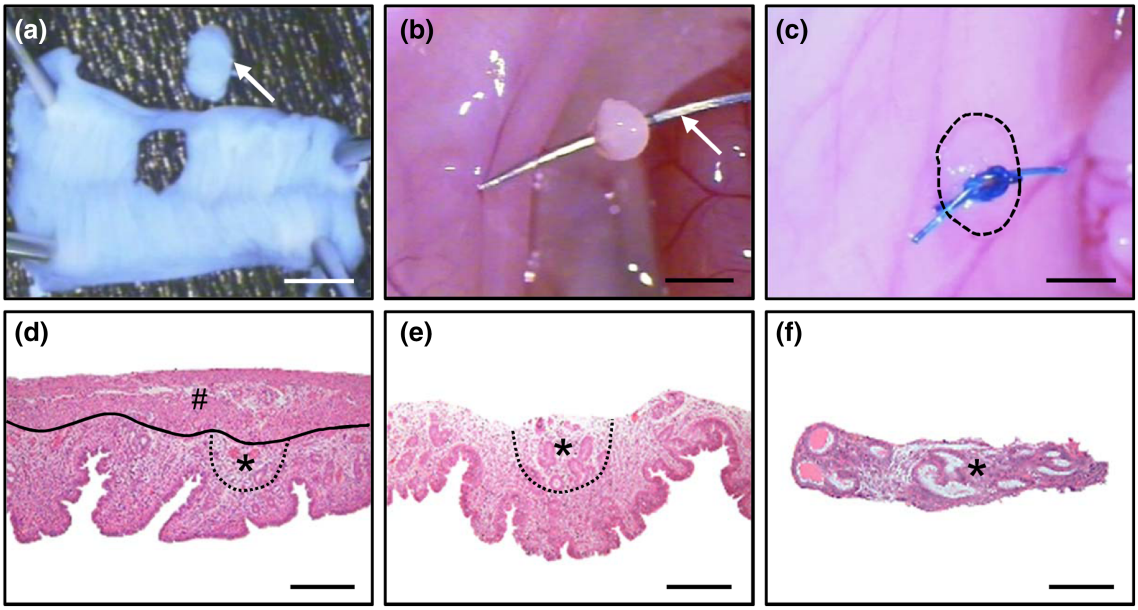

FIGURE 1 (a) Longitudinally opened uterine horn of a BALB/c donor mouse with a 2-mm tissue sample (arrow), which was excised by means of a 2-mm dermal biopsy punch. (b) Fixation of the tissue sample to the abdominal wall of a BALB/c recipient mouse for the induction of a peritoneal endometriotic lesion (arrow: needle of the Prolene suture). (c) Typical appearance of the transplant (border marked by broken line) directly after fixation. Scale bars: 2.5 mm. (d–f) HE-stained tissue sections illustrating the preparation of endometrial fragments, which were transplanted into the dorsal skinfold chamber of BALB/c recipient mice. For this purpose, the perimetrium and myometrium (in d; shown as #; line = border to the underlying endometrium) were removed from fixed, longitudinally opened uterine horns by means of microsurgical instruments under a stereo-microscope. Circular tissue fragments (d–f; shown as *, border marked by dotted line), which only consisted of endometrial stroma and glands (f), were then excised from the underlying endometrium. Scale bars: d, e = 240 µm; f = 120 µm

2.4 | High-resolution ultrasound imaging and analysis

The development of peritoneal endometriotic lesions was repetitively analyzed with a Vevo 770™ high-resolution ultrasound imaging system (VisualSonics, Toronto, ON, Canada) by means of a real-time microvisualization (RMV™) 704 Scanhead (VisualSonics) with a centre frequency of 40 MHz and a focal depth of 6 mm (Laschke et al., 2010). For this purpose, the mice were anaesthetized with 2% isoflurane in oxygen, fixed in a supine position on a heated stage and the abdomen was chemically depilated (Nair hair removal lotion; Church & Dwight Canada Corp., Mississauga, ON, Canada). A three-dimensional reconstruction and analysis software from VisualSonics (Vevo 770 V2.3.0) was used to analyze the ultrasound images. To measure the overall volume of developing endometriotic lesions as well as the volume of their stromal tissue and cysts (in mm^3) by manual image segmentation, boundaries of the lesions and their cysts were outlined in parallel slices with a step size of 200 μm (Rudzitis-Auth et al., 2020). Moreover, we calculated the growth of lesions and stromal tissue (in % of the initial lesion and stromal tissue size) and assessed the number of cyst-containing lesions (in %).

At the end of the in vivo experiments, the anaesthetized animals were carefully laparotomized under a stereo-microscope and the largest (D1) and perpendicularly aligned diameter (D2) of the endometriotic lesions were measured by means of a digital calliper. The lesion size (S) was then calculated by $S = D1 * D2 * \pi/4$ (Becker et al., 2008). Furthermore, the lesions as well as the ovaries and uterine horns were harvested and fixed in formalin for additional histological and immunohistochemical analyses.

2.5 | Dorsal skinfold chamber model

To further investigate the effect of SPHK1 inhibition on the early vascularization of endometriotic lesions, a mouse dorsal skinfold chamber model was used. This well established model allows the repetitive monitoring of the newly developing microvasculature in endometriotic lesions by means of intravital fluorescence microscopy (Laschke et al., 2011). For this purpose, the two titanium frames of the dorsal skinfold chamber, sandwiching the dorsal skinfold, were implanted onto the back of mice in the stage of dioestrus, as described previously in detail (Laschke et al., 2011). Thereafter, the animals received a s.c. injection of 5-mg kg^{-1} carprofen as pain medication and were allowed to recover from anaesthesia and surgical trauma for 48 h (i.e., until the stage of oestrus). The feeding, cleaning and sleeping habits as well as the mobility of the mice was not impaired by the implantation of the dorsal skinfold chamber.

For the generation of endometrial fragments, BALB/c mice in the stage of oestrus were anaesthetized by i.p. injection of ketamine (75 mg kg^{-1}) and xylazine (15-mg kg^{-1}). The two uterine horns were excised, placed in a petri dish containing DMEM (10% FCS, 100 U ml^{-1} penicillin, 0.1 mg ml^{-1} streptomycin) and opened longitudinally (Figure 1d). Subsequently, the tissue was fixed on a sterile cork plate and the perimetrium and myometrium were carefully removed by means of microsurgical instruments under a stereo-microscope (M651; Leica Microsystems, Wetzlar, Germany) (Figure 1e). From the underlying endometrium, circular fragments with a diameter of ~0.8 mm were then excised (Figure 1f) and stained for 30 s with the fluorescent dye Hoechst 33342 (200 μg ml^{-1}). Thereafter, two fragments were placed onto the striated muscle tissue within the observation window of each dorsal skinfold chamber.

2.6 | Intravital fluorescence microscopy

For the analysis of microcirculatory parameters, the vascularization of the grafted endometrial fragments was observed directly after transplantation (d0) as well as on day 3, 6, 10 and 14 by means of intravital fluorescence microscopy. For this purpose, the anaesthetized mice received an i.v. injection of 0.1 ml 5% FITC-labelled dextran (150,000 Da) into the retrobulbar venous plexus. This enhanced the blood vessel contrast by staining of the intravascular blood plasma. The mice were then placed on a plexiglas stage and the newly developing microvessels were visualized by means of a Zeiss Axiotech microscope (Zeiss, Oberkochen, Germany) equipped with a 100-W mercury lamp attached to a filter block for blue, green and UV light. The microscopic images were recorded by a charge-coupled device video camera (FK6990; Pieper, Schwerte, Germany) and transferred to a DVD system for off-line evaluation. The recorded images were quantitatively analyzed by means of CapImage (version 8.5; Zeintl, Heidelberg, Germany). This included the determination of the size of the endometrial fragments (mm^2), their functional microvessel density (cm cm^{-2}) as well as the diameters (μm) of 20 individual microvessels per lesion, their centerline red blood cell (RBC) velocity (μm s^{-1}) and volumetric blood flow (pL s^{-1}) (Laschke, Vorsterman van Oijen, et al., 2011).

2.7 | Histology and immunohistochemistry

Formalin-fixed specimens of peritoneal endometriotic lesions, ovaries and uterine horns were embedded in paraffin. Sections (3 μm) were cut and stained with haematoxylin and eosin (HE) according to standard procedures.

For the immunohistochemical detection of proliferating cells and hypoxic cells, sections were stained with a rabbit polyclonal antibody against the proliferation marker Ki67 (1:100) or a rabbit polyclonal antibody against the hypoxia marker HIF-1α (1:50). A goat anti-rabbit biotinylated antibody (ready-to-use) followed by avidin-peroxidase (1:50) or a goat anti-rabbit peroxidase-labelled antibody (1:100) served as secondary antibody. 3-Amino-9-ethylcarbazole (AEC Substrate System) was used as chromogen and counterstaining was performed with hemalaun. The fraction of proliferating cells and hypoxic cells (%) was assessed by counting the numbers of $Ki67^+$ and $HIF\text{-}1\alpha^+$ cells in four regions of interest within the tissue.

For the immunofluorescent detection of microvessels, sections were stained with a monoclonal rat anti-mouse antibody against the endothelial cell marker CD31 (1:100). A goat anti-rat IgG Alexa555 antibody served as secondary antibody (1:200). Cell nuclei were stained with Hoechst 33342 (2 μg ml^{-1}). The microvessel density (mm^{-2}) was measured using a BZ-8000 microscope (Keyence, Osaka, Japan). For this purpose, the overall number of $CD31^+$ microvessels was counted and divided by the area of stromal tissue.

The Immuno-related procedures used comply with the recommendations made by the British Journal of Pharmacology (Alexander et al., 2018).

2.8 | Experimental protocol

In a first set of experiments, a total of 60 uterine tissue samples (= technical replicates) from 4 donor mice were transplanted into 15 recipient mice (= biological replicates) by fixation of two grafts at the right and left wall of the abdomen. The animals were divided into two groups receiving daily either 10 mg kg^{-1} SKI-5C (n = 7) or 0.1-ml corn oil as vehicle (control; n = 8) by i.p. injection for 28 days. The lower number of animals in the SKI-5C-treated group was caused by the death of a mouse during anaesthesia. This dose of SKI-5C has previously been shown to effectively inhibit the vascularization of breast cancer xenografts (Datta et al., 2014). Directly after tissue transplantation (d0) as well as on days 7, 14, 21 and 28 the newly developing endometriotic lesions were analyzed by means of high-resolution ultrasound imaging. At the end of the in vivo experiments, the size of the lesions was measured by means of a digital calliper. Subsequently, the lesions, uterine horns and ovaries were excised for further histological and immunohistochemical analyses.

In a second set of experiments, a total of 68 uterine tissue samples (= technical replicates) from four donor mice were transplanted into 17 recipient mice (= biological replicates), which were treated daily with either 10 mg kg^{-1} SKI-5C i.p. (n = 9) or vehicle i.p. (control; n = 8) for 7 days, as described above. The lower number of animals in the SKI-5C-treated group was caused by the death of a mouse during anaesthesia. Subsequently, the lesions, uterine horns and ovaries were excised for further histological and immunohistochemical analyses.

In a third set of experiments, a total of 24 endometrial fragments (= technical replicates) from four donor mice were transplanted into the dosal skinfold chambers of 12 recipient mice (= biological replicates), which were treated daily with either 10 mg kg^{-1} SKI-5C i.p. (n = 6) or vehicle i.p. (control; n = 6) for 14 days, as described above. Intravital fluorescence microscopy of the grafts was performed directly after tissue transplantation (d0) as well as on days 3, 6, 10 and 14.

2.9 | Data and statistical analysis

The data and statistical analysis comply with the recommendations on experimental design and analysis in pharmacology (Curtis et al., 2018). All experiments were designed to generate groups of equal size, using randomization and blinded analysis. The statistical analysis was undertaken only for experiments where each group size was at least n = 5 of independent values and performed using these independent values.

The group sizes for the in vivo experiments were chosen according to previous studies using the herein described endometriosis models (Rudzitis-Auth et al., 2020). Data were first analyzed for normal distribution and equal variance. In case of parametric data, differences between two experimental groups were assessed by the unpaired Student's t test. In case of non-parametric data, differences between two experimental groups were assessed by the Mann–Whitney rank sum test (SigmaPlot 13.0; Jandel Corporation, San Rafael, CA, USA, RRID:SCR_003210). All data are given as mean ± SEM. Statistical significance was accepted for $P < 0.05$.

2.10 | Materials

SKI-5C (2,2-dimethyl-4S-(1-oxo-2-hexadecyn-1-yl)-1,1-dimethylethyl ester-3-oxazolidinecarboxylic acid), corn oil, FITC-labeledlabelled dextran, Hoechst 33342 were from Sigma-Aldrich (Taufkirchen, Germany). DMEM was from PAN-Biotech (Aidenbach, Germany). FetalFoetal calf serum (FCS), penicillin and streptomycin were from Biochrom (Berlin, Germany). Ketamine was from Serumwerke Bernburg (Bernburg, Germany). Xylazine was from Bayer AG (Leverkusen, Germany). Rimadyl (carprofen) was from Zoetis Deutschland GmbH (Berlin, Germany). Dorsal skinfold chambers were from Irola Industriekomponenten GmbH & Co. KG (Schonach, Germany). Dermal biopsy punches were from Stiefel Laboratorium GmbH (Offenbach am Main, Germany). Prolene sutures were from Ethicon Products (Norderstedt, Germany). The monoclonal rat anti-mouse antibody against CD31 (Cat# DIA-310, RRID:AB_2631039) was from Dianova (Hamburg, Germany) and its corresponding goat anti-rat IgG Alexa555 secondary antibody (Cat# A-21434, RRID:AB_2535855) was from Thermo Fisher Scientific (Dreieich, Germany). The rabbit polyclonal antibody against Ki67 (Cat# ab15580, RRID:AB_443209) and its corresponding goat anti-rabbit biotinylated secondary antibody (Cat# ab64256, RRID:AB_2661852), the rabbit polyclonal antibody against hypoxia-inducible factor (HIF)-1α (Cat# ab114977, RRID:AB_10900336) and its corresponding goat anti-rabbit peroxidase-labeledlabelled secondary antibody (Cat# 111-035-04, RRID:AB_2307391) as well as 3-amino-9-ethylcarbazole (AEC Substrate System; Cat# ab64252, RRID:AB_2336076) were from Abcam (Cambridge, UK).

2.11 | Nomenclature of targets and ligands

Key protein targets and ligands in this article are hyperlinked to corresponding entries in the IUPHAR/BPS Guide to PHARMACOLOGY (http://www.guidetopharmacology.org) and are permanently archived in the Concise Guide to PHARMACOLOGY 2019/20

(Alexander, Christopoulos, et al., 2019; Alexander, Cidlowski, et al., 2019; Alexander, Fabbro, et al., 2019a, 2019b; Alexander, Kelly, et al., 2019a, 2019b).

3 | RESULTS

3.1 | Growth and cyst formation of endometriotic lesions

The development of peritoneal endometriotic lesions was analyzed by means of repetitive high-resolution ultrasound imaging throughout an observation period of 28 days (Figure 2a,b). Directly after the transplantation of uterine tissue samples from donor mice to the abdominal wall of recipient animals, the grafts exhibited a comparable initial size of ~1.5 mm^3 in the vehicle- and the SKI-5C-treated group (Figure 2c). During the following time course, the volume of newly developing endometriotic lesions in the vehicle-treated mice progressively increased, whereas the lesion growth in the SKI-5C-treated animals was significantly suppressed (Figure 2c,d). Accordingly, SKI-5C-treated lesions also presented with a reduced stromal tissue volume and stromal tissue growth on days 21 and 28 when compared to controls (Figure 2e,f). Moreover, their cyst volume was markedly reduced at the end of the 28-days observation period, while the final fraction

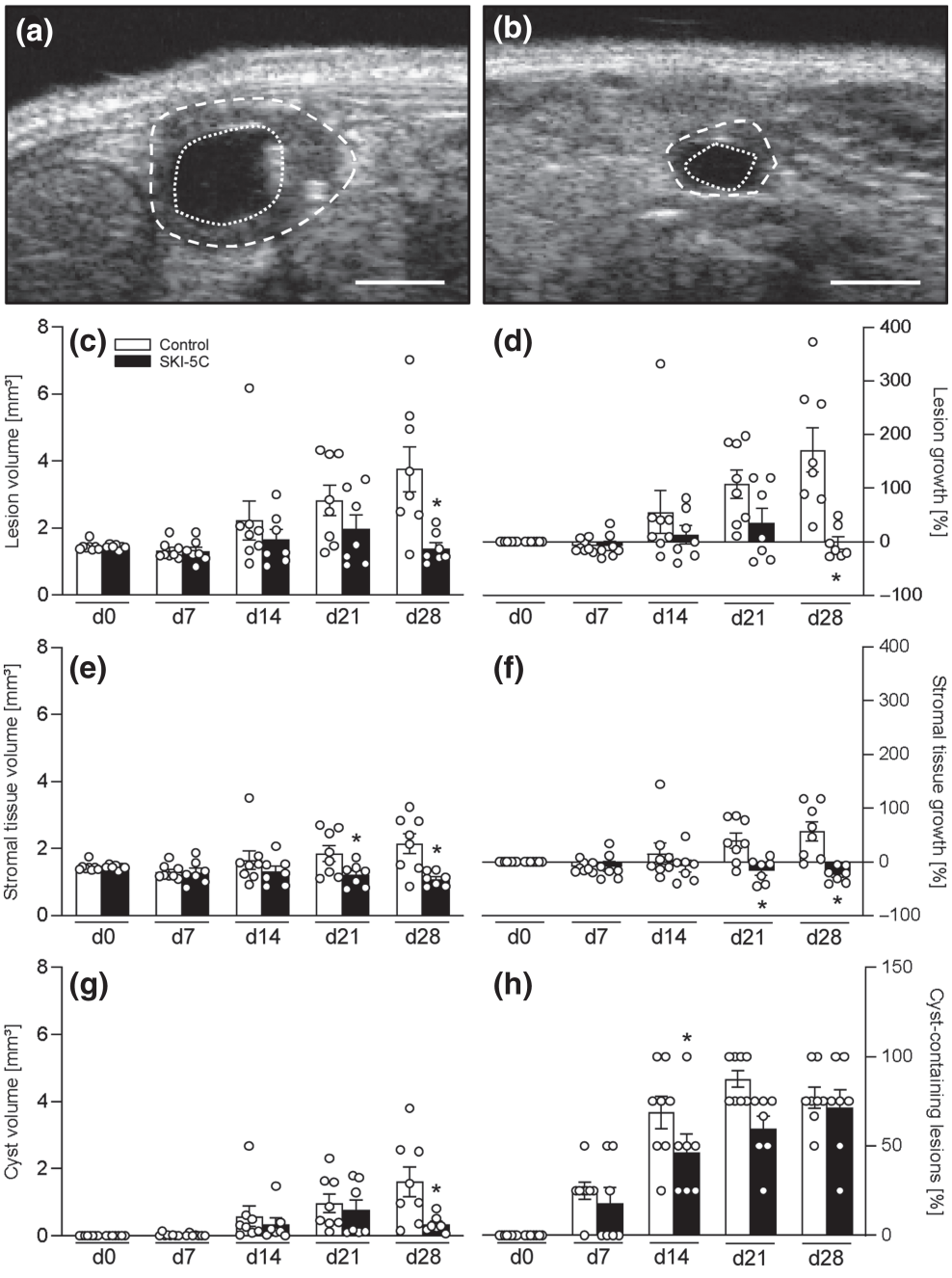

FIGURE 2 (a,b) High-resolution ultrasound imaging of newly developed endometriotic lesions (border marked by broken line, cyst-like dilated endometrial glands marked by dotted line) 28 days after transplantation of uterine tissue samples to the abdominal wall of a vehicle-treated control (a) and a SKI-5C-treated BALB/c mouse (b). Scale bars: a, b = 1 mm. (c–h) Overall lesion volume (c, mm^3), lesion growth (d, %), stromal tissue volume (e, mm^3), stromal tissue growth (f, %), cyst volume (g, mm^3) and fraction of cyst-containing lesions (h, %) of endometriotic lesions in vehicle-treated controls ($n = 8$) and SKI-5C-treated BALB/c mice ($n = 7$), as assessed by high-resolution ultrasound imaging on days 7, 14, 21 and 28. Data shown are individual values with means ± SEM. *$P < 0.05$, significantly different from control

of cyst-containing lesions was comparable in both groups (Figure 2g, h). In line with these results, additional histological analyses on day 28 revealed that SKI-5C-treated endometriotic lesions also contained smaller cyst-like dilated glands (Figure 3a,b). Moreover, they exhibited a significantly lower caliper-assessed lesion size when compared with vehicle-treated controls (Figure 3c).

3.2 | Vascularization and cell proliferation of endometriotic lesions

Immunohistochemical analyses revealed a significantly lower density of $CD31^+$ microvessels within SKI-5C-treated peritoneal endometriotic lesions on day 7 when compared to vehicle-treated controls (Figures 4a, 4b and 4m). In contrast, the lesions of both groups exhibited a comparable microvessel density on day 28 (Figures 4c, 4d and 4m). These results demonstrate that the blockade of SPHK1 inhibits the formation of new microvascular networks, particularly in the early phase of lesion development.

In addition, we found that vehicle- and SKI-5C-treated lesions contained a comparably high number of proliferating $Ki67^+$ stromal and glandular cells on day 7 (Figures 4e, 4f and 4n). On day 28, the lesions of both groups exhibited markedly lower numbers of proliferating stromal and glandular cells (Figure 4n). Moreover, stromal cell proliferation was significantly reduced in SKI-5C-treated lesions at this late time point when compared to vehicle-treated controls (Figures 4g, 4h and 4n). Finally, we only detected a low fraction of HIF-$1\alpha^+$ stromal cells on day 7 and 28, which did not significantly differ between the two groups (Figures 4i–l and 4o).

3.3 | Effect of SPHK1 inhibition on the female reproductive organs

To detect potential side effects of SPHK1 inhibition on the female reproductive organs, we additionally analyzed the vascularization and proliferation within the ovaries and uterine horns of vehicle- and SKI-5C-treated animals on day 7 and 28 after the surgical induction of endometriotic lesions. Notably, there were no significant differences in the microvessel density and the number of proliferating cells between the two groups (Figure 5a–k).

3.4 | Early vascularization of endometriotic lesions in the dorsal skinfold chamber

Finally, we used the dorsal skinfold chamber model to analyze the effect of SPHK1 inhibition on the early vascularization of endometriotic lesions by means of intravital fluorescence microscopy. This approach does not only allow the assessment of the morphology of newly developing microvascular networks, but also the measurement of microhaemodynamic parameters (Laschke, Vorsterman van Oijen, et al., 2011). Consistent with the results of our peritoneal endometrosis model, we found that the treatment with SKI-5C suppressed the growth of newly developing endometriotic lesions during the observation period of 14 days (Figure 6a–c). In addition, endometriotic lesions in SKI-5C-treated mice exhibited a significantly lower functional microvessel density between day 6 to day 14, when compared with the lesions in vehicle-treated control animals (Figures 6a, 6b and 6d). Moreover, microvessels within SKI-5C-treated lesions presented with significantly smaller diameters and a reduced volumetric blood flow on day 10 (Table 1).

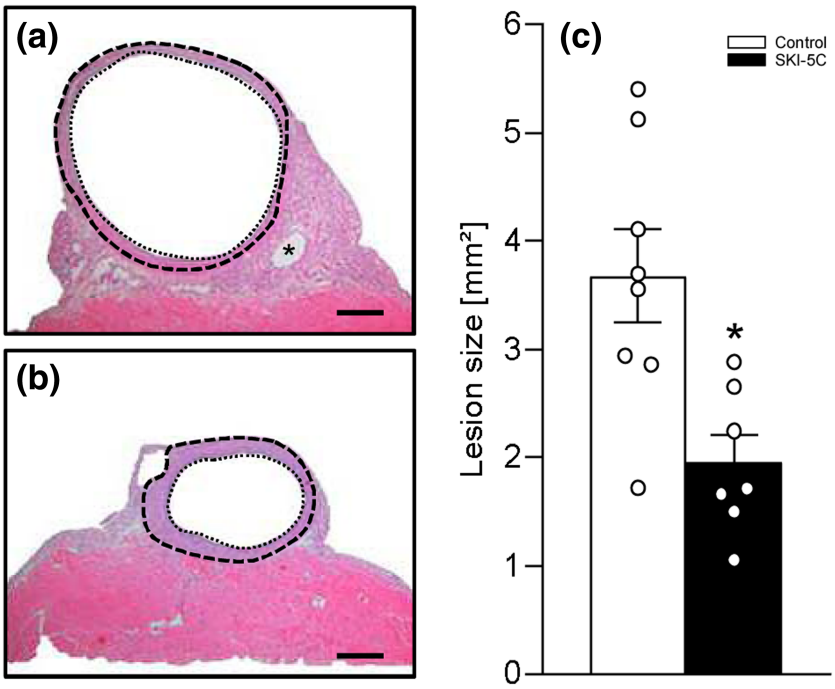

FIGURE 3 (a,b) HE-stained endometriotic lesions (border marked by broken line, cyst-like dilated endometrial glands marked by dotted line, asterisk = suture) 28 days after transplantation of uterine tissue samples to the abdominal wall of a vehicle-treated control (a) and a SKI-5C-treated BALB/c mouse (b). Scale bars: a, b = 250 μm. (c) Lesion size (mm^2) of endometriotic lesions in vehicle-treated controls ($n = 8$) and SKI-5C-treated BALB/c mice ($n = 7$), as assessed by caliper measurements. Data shown are individual values with means ± SEM. *$P < 0.05$, significantly different from control

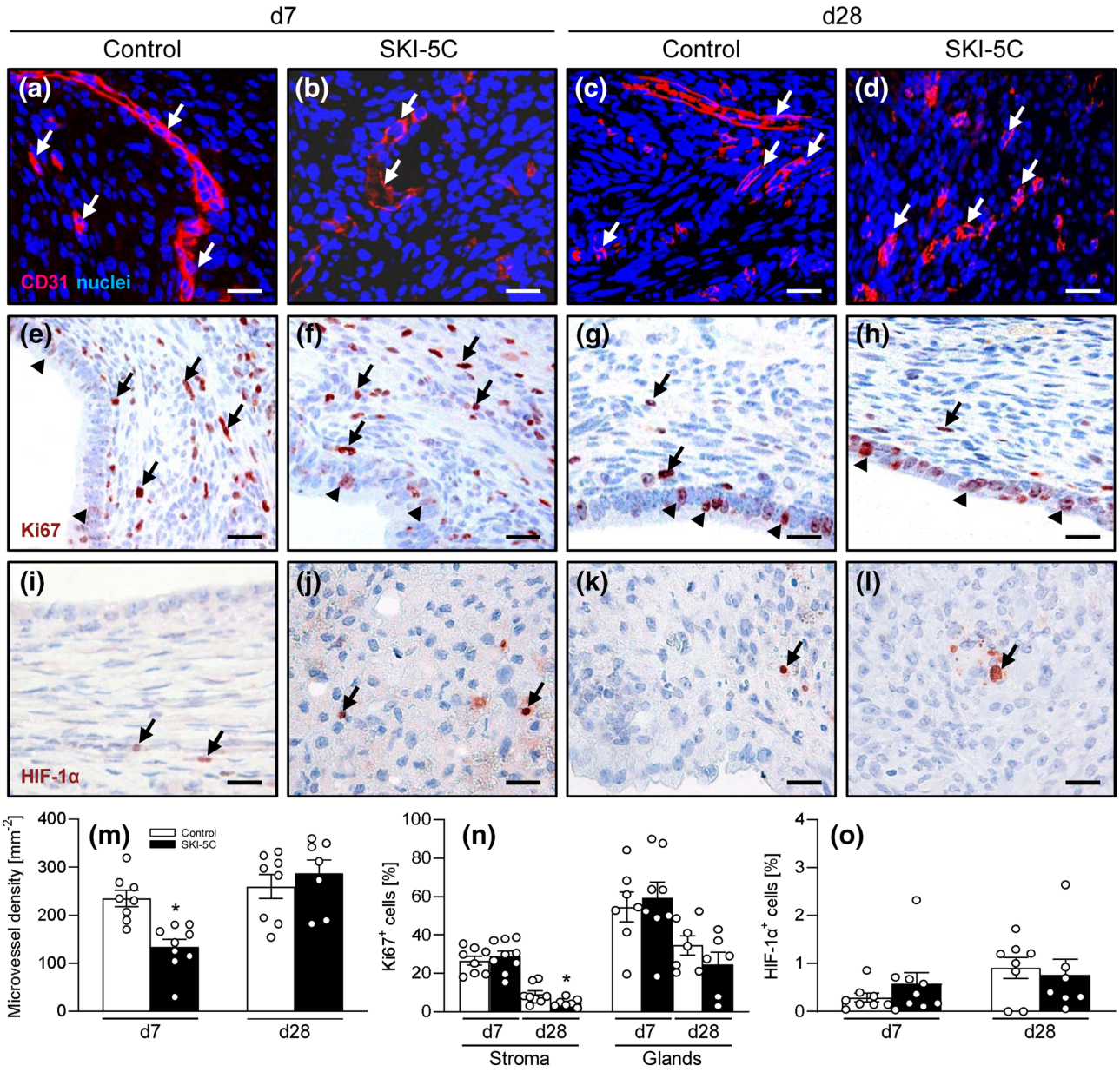

FIGURE 4 (a–d) Immunofluorescent detection of CD31$^+$ microvessels (arrows) on day 7 and 28 after transplantation of uterine tissue samples to the abdominal wall of vehicle-treated controls and SKI-5C-treated BALB/c mice. Scale bars: 40 μm. (e–h) Immunohistochemical detection of proliferating Ki67$^+$ stromal cells (arrows) and glandular epithelial cells (arrowheads) on day 7 and 28 after transplantation of uterine tissue samples to the abdominal wall of vehicle-treated controls and SKI-5C-treated BALB/c mice. Scale bars: 40 μm. (i–l) Immunohistochemical detection of hypoxic HIF-1α$^+$ stromal cells (arrows) on day 7 and 28 after transplantation of uterine tissue samples to the abdominal wall of vehicle-treated controls and SKI-5C-treated BALB/c mice. Scale bars: 40 μm. M: Microvessel density (mm^{-2}) of endometriotic lesions in vehicle-treated controls (n = 8–9) and SKI-5C-treated BALB/c mice (n = 7–9), as assessed by immunohistochemistry. Data shown are individual values with means ± SEM. *P < 0.05, significantly different from control. N: Ki67$^+$ cells (%) within the stroma and the glands of endometriotic lesions in vehicle-treated controls (n = 8–9) and SKI-5C-treated BALB/c mice (n = 7–9), as assessed by immunohistochemistry. Data shown are individual values with means ± SEM. *P < 0.05, significantly different from control O: HIF-1α$^+$ cells (%) within the stroma of endometriotic lesions in vehicle-treated controls (n = 8) and SKI-5C-treated BALB/c mice (n = 7–9), as assessed by immunohistochemistry. Data shown are individual values with means ± SEM

4 | DISCUSSION

An increasing number of studies suggests that sphingolipids, such as S1P, are involved in the pathogenesis of endometriosis. In fact, S1P promotes the growth of endometriotic cells through the overexpression of IL-6 a pro-inflammatory cytokine associated with the establishment of endometriotic lesions (Bergqvist et al., 2001). Moreover, the expression of several enzymes involved in the cellular maintenance of balanced S1P levels is deregulated in endometriotic lesions (Santulli et al., 2012). This mainly affects enzymes responsible

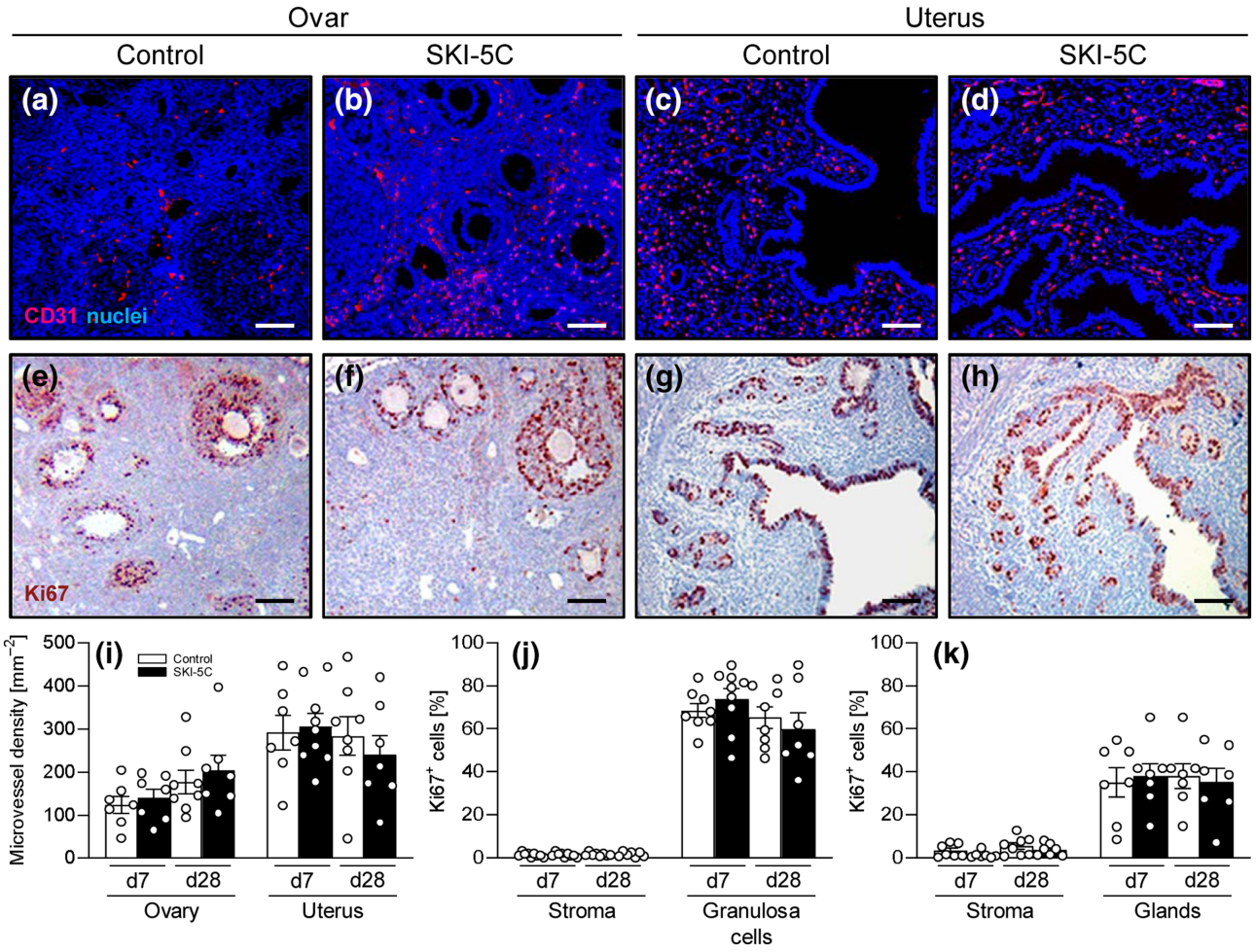

FIGURE 5 (a–h) Immunohistochemical detection of CD31$^+$ microvessels (a–d) and proliferating Ki67$^+$ cells (e–h) in the ovaries (a, b, e and f) and uterine horns (c, d, g and h) on day 28 after transplantation of uterine tissue samples to the abdominal wall of vehicle-treated controls (a, c, e and g) and SKI-5C-treated (b, d, f and h) BALB/c mice. Scale bars: 80 μm. (i) Microvessel density (mm^{-2}) of the ovaries and uterine horns in vehicle-treated controls ($n = 7–9$) and SKI-5C-treated BALB/c mice ($n = 7–9$), as assessed by immunohistochemistry. Mean ± SEM. J, K: Ki67$^+$ cells (%) within the stroma and the follicles of the ovaries (j) as well as the stroma and glands of the uterine horns (k) in vehicle-treated controls ($n = 7–9$) and SKI-5C-treated BALB/c mice ($n = 7–9$), as assessed by immunohistochemistry. Data shown are individual values with means ± SEM

for the inactivation of S1P, resulting in an accumulation of the sphingolipid within the cells. S1P, in turn, acts as a chemoattractant for endothelial cells via the **S1P$_1$ receptor** and stimulates their proliferation and migration (Hla et al., 2001). Furthermore, the activation of S1P$_1$ receptors by S1P maintains the vascular stability and barrier function during blood vessel development (Hisano & Hla, 2019). In contrast, inhibition of SPHK1 and, consequently, low levels of endogenous S1P provoke an endothelial hypersprouting phenotype in vitro (Gaengel et al., 2012). This is associated with the insufficient recruitment of mural cells, which results in a malformation of the microvasculature. Accordingly, several studies indicate that the pharmacological inhibition of SPHK1 suppresses the development of functional microvascular networks in different pathological conditions (Ader et al., 2015; Dai et al., 2017). As angiogenesis has been identified as a major prerequisite for the establishment and progression of endometriotic lesions inside the abdominal cavity, anti-angiogenic approaches have been suggested as a potential treatment strategy in the management of endometriosis (Bedaiwy et al., 2017). Consistent with this view, we could demonstrate in the present study that blockade of SPHK1 by the low MW inhibitor SKI-5C inhibited the vascularization and growth of newly developing endometriotic lesions.

For our study, we used a well-established mouse model of peritoneal endometriosis (Kiani et al., 2019; Rudzitis-Auth et al., 2020). In this model, endometriotic lesions are surgically induced by transplanting uterine tissue samples from donor mice to the abdominal wall of syngeneic recipient animals. Although this is a widely used model in endometriosis research, which has been proven to be suitable for the assessment of pharmacological effects on endometriotic lesions, it has to be considered that it does not involve the use of pathological endometriotic tissue derived from humans. Accordingly, the results obtained in the present study may not fully relate to human patients with endometriosis. In fact, human endometriotic lesions originate from menstruated endometrial tissue, while mice do not menstruate and, thus, do not develop spontaneous endometriosis. To overcome

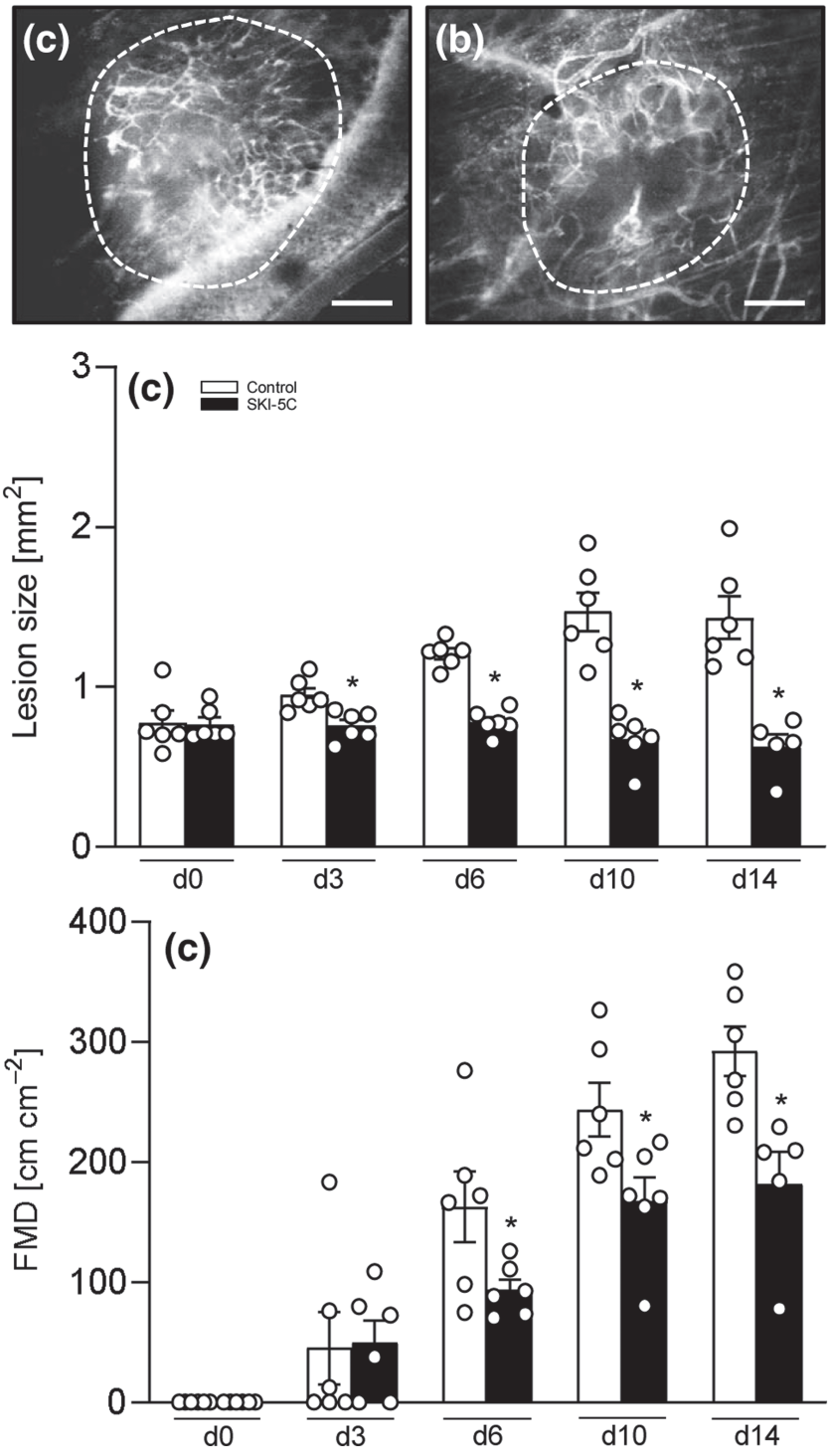

FIGURE 6 (a,b) Intravital fluorescent microscopic images of newly developed endometriotic lesions (borders marked by broken line) on day 10 after transplantation of endometrial fragments into the dorsal skinfold chamber of a vehicle-treated control (a) and a SKI-5C-treated BALB/c mouse (b). Scale bars: 175 μm. (c,d) Lesion size (mm^2; c) and functional microvessel density (FMD; cm cm^{-2}; d) of endometriotic lesions in dorsal skinfold chambers of vehicle-treated controls ($n = 6$) and SKI-5C-treated BALB/c mice ($n = 6$), as assessed by intravital fluorescence microscopy. Data shown are individual values with means ± SEM. *$P < 0.05$, significantly different from control

this problem, novel approaches have recently been established to induce decidualization of the endometrium in mice (Peterse et al., 2018). Greaves et al. (2014, 2017) found that endometriotic lesions originating from decidualized mouse endometrium exhibit many similarities to human endometriotic lesions regarding expression of **oestrogen receptor**s, inflammation, macrophage infiltration and pain induction. Nonetheless, even the direct transfer of findings from such menstruating mouse models to the human situation is questionable, because the signalling processes involved in decidualization are different in both species (Ramathal et al., 2010).

Our ultrasound analyses revealed that the lesions in vehicle-treated control mice progressively grow during the observation period of 28 days, whereas lesion growth is significantly inhibited in SKI-5C-treated animals. To clarify whether this was caused by hypoxia resulting from the impaired vascularization of SKI-5C-treated lesions, we performed immunohistochemical staining of the lesions with the

	d3	d6	d10	d14
Diameter (μm)				
Control	16.8 ± 1.2	15.4 ± 0.6	16.0 ± 1.2*	15.1 ± 0.9*
SKI-5C	18.4 ± 0.4*	15.0 ± 1.0	12.6 ± 0.7*	12.8 ± 1.2
Centerline RBC velocity (μm s^{-1})				
Control	122.1 ± 19.5	223.3 ± 43.0	187.8 ± 39.3	180.5 ± 32.4
SKI-5C	75.6 ± 25.9	103.0 ± 17.5	158.3 ± 29.8	176.4 ± 39.0
Volumetric blood flow (pL s^{-1})				
Control	20.1 ± 3.5	28.1 ± 4.9	30.3 ± 6.4	28.8 ± 7.8
SKI-5C	23.0 ± 8.7	14.4 ± 3.1	15.6 ± 3.4*	17.5 ± 4.6

Data shown are means ± SEM (n=6 for both groups). RBC: red blood cell. d3, d6, d10, d14 refer to day3 – day14 of the study.
*P < 0.05, significantly different from control values.

TABLE 1 Diameter, centerline RBC velocity and volumetric blood flow of individual microvessels within endometriotic lesions in dorsal skinfold chambers of vehicle-treated controls (n = 6) and SKI-5C-treated BALB/c mice (n = 6), as assessed by intravital fluorescence microscopy and computer-assisted image analysis throughout an observation period of 14 days

well-established hypoxia marker HIF-1α. Of interest, we found that the lesions of both groups contained only a very low fraction of hypoxic stromal cells on day 7 and 28 after induction. This finding implies that other mechanisms than hypoxia must have been involved in mediating the inhibitory effects of the SPHK1 inhibitor SKI-5C on lesion growth and stromal cell proliferation. In this context, it has already been reported that the inhibition of S1P signaling, via $S1P_1$ and **$S1P_3$** receptors, directly suppresses the proliferation of endometrial stromal cells (Yoshino et al., 2019). Moreover, Datta et al. (2014) found that SKI-5C increases cell cycle arrest in the G1 phase in triple-negative breast cancer cells, which is associated with a decreased phosphorylation of **ERK1/2** and **Akt**. Additional studies in tumour cell lines and breast epithelial cells indicate that the anti-proliferative effect of SPHK1 inhibition may also be caused by a reduced expression of NF-κB (Li et al., 2014, 2016). In endometriotic lesions, NF-κB activation enhances cell proliferation and survival (González-Ramos et al., 2010). Conversely, inhibition of NF-κB has been shown to suppress DNA synthesis and to induce apoptosis and cell cycle arrest in endometriotic stromal cells by inhibiting the phosphorylation of the IκB protein, resulting in the regression of endometriotic lesions in vivo (González-Ramos et al., 2008; Nasu et al., 2007).

In addition, recent studies suggest that S1P increases **COX-2** mRNA expression and, thus, enhances the secretion of **PGE_2** (Rumzhum et al., 2016). SPHK1 deficiency, in turn, is associated with a reduced COX-2 expression (Furuya et al., 2017). These are interesting observations considering the fact that COX-2/PGE_2 signalling has been shown to regulate the secretory activity of endometrial glands (Rudzitis-Auth et al., 2018). Moreover, others have demonstrated that SPHK1 is localized in glandular epithelial cells and that the concentration of S1P is increased in the cyst fluid of endometriomas (Yoshino et al., 2019). In line with these findings, we found significantly lower cyst volumes in endometriotic lesions of SKI-5C-treated mice when compared with controls.

The maintenance and formation of adherence junctions in the microvasculature is mediated by S1P-induced activation of $S1P_1$ receptors (Blaho & Hla, 2014). Moreover, S1P promotes endothelial cell migration and VEGF-induced vessel formation (Lee et al., 1999). In addition, $S1P_1$ receptors are necessary for the stabilization of blood vessels. Hence, knock-down of this receptor causes extensive vascular haemorrhages and a lethal phenotype in mice lacking $S1P_1$ receptors (Liu et al., 2000). The same effects are observed in SPHK1- and SPHK2-double knockout mice (Mizugishi et al., 2005). This indicates that S1P represents a promising target for anti-angiogenic therapy. Accordingly, the treatment with a specific monoclonal antibody against S1P inhibited vessel formation and induced tumour regression in multiple murine cancer models (Visentin et al., 2006). In vitro and in vivo assays revealed that this was associated with a reduced release of the pro-angiogenic factors IL-6, **IL-8** and VEGF (O'Brien et al., 2009; Visentin et al., 2006). Thus, it is possible that these mechanisms also caused the lower microvessel density within SKI-5C-treated endometriotic lesions, compared with vehicle-treated controls, that we detected here. Of interest, this effect of SPHK1 inhibition was only observed on day 7. This may be explained by the fact that in the present experimental setting, the uterine tissue grafts lack their own blood supply and, thus, suffer from hypoxia until day 3 after transplantation (Laschke, Giebels, et al., 2011). Hypoxia, in turn, is a major trigger for the cellular release of S1P (Ader et al., 2009). Hence, the anti-angiogenic action of SKI-5C on endometriotic lesions may be mainly effective in the early phase of lesion development. Taking this into account, future clinical treatment with a SPHK1 inhibitor may be particularly suitable to suppress the establishment of new endometriotic lesions with a high angiogenic activity after surgical treatment, preventing the recurrence of the disease.

In an additional set of experiments, we analyzed the early vascularization of endometriotic lesions in the dorsal skinfold chamber model. This model allows the repetitive in vivo assessment of morphological and microhaemodynamic parameters during the formation of new microvascular networks within the same animals over time, which markedly reduces the number of animals required for the analysis, thus complying with the 3Rs principles (Laschke, Vorsterman van Oijen, et al., 2011). Transplanted endometrial fragments progressively grew in vehicle-treated control mice, whereas the grafts in SKI-5C-treated animals even decreased in size over time. Furthermore, the functional microvessel density of SKI-5C-treated

lesions was significantly lower between days 6–14, compared with controls. The latter finding is in line with the results of our peritoneal endometriosis model, in which we also observed a reduced microvessel density in SKI-5C-treated lesions on day 7. In contrast, the lesions of both groups exhibited a comparable density of $CD31^+$ microvessels on day 28. This may be explained by a completed engraftment process at this late time point. Hence, although we detected a delayed vascularization under SKI-5C treatment, at the end of the experiment, the lesions of the two groups no longer differed in terms of microvessel density.

In adults, physiological angiogenesis typically occurs in the female reproductive system (Reynolds et al., 2002). In this context, it should be noted that S1P in follicular fluid stimulated the proliferation of endothelial cells and blood vessel formation during the development of ovarian follicles (von Otte et al., 2006). Additionally, S1P signalling is involved in the decidualization of human endometrial stromal cells and the disruption of both SPHK genes leads to defects in decidual blood vessels (Brünnert et al., 2014; Mizugishi et al., 2007). Hence, we further investigated whether SKI-5C treatment induced side effects in the uterus and ovaries. Notably, we found that these organs did not differ in terms of morphology, vascularization and proliferative activity between vehicle- and SKI-5C-treated mice. These preliminary results indicate that the pharmacological inhibition of SPHK1 suppresses the development of endometriotic lesions without affecting the physiological function of the female reproductive organs. In line with these findings, SPHK1- or SPHK2-knockout mice are viable and fertile with no obvious phenotypic changes (Kunkel et al., 2013). This indicates that a reduced synthesis of S1P by loss or suppression of the activity of one of the two enzymes seems to be compensated by a higher activity or up-regulation of the non-affected enzyme (Mizugishi et al., 2005). Based on our results, it is likely that this compensatory mechanism still works properly in the female reproductive organs during treatment with SKI-5C, while it is disabled under the pathological conditions of ectopic lesion formation.

Finally, it should be considered that the local synthesis of **oestrogen** by overexpression of aromatase (**CYP19A1**, Cytochrome P450 Family 19 Subfamiliy A Member 1) and steroidogenic acute regulatory protein (**StaR**) plays a major role in the establishment and progression of endometriosis (Attar et al., 2009). Moreover, the activation of the two oestrogen receptor isoforms **ERα** and **ERβ** is required for the growth of endometriotic lesions (Burns et al., 2012; Zhao et al., 2015). Recent studies suggest that oestrogen activates SPHK1 (Sukocheva et al., 2015). This promotes S1P synthesis and $S1P_1$ receptor-mediated angiogenesis (Young & Van Brocklyn, 2006). Hence, although not further analyzed in the present study, it may be assumed that the inhibition of SPHK1 also suppresses the establishment of endometriotic lesions via blockade of oestrogen receptor signalling.

In summary, we have demonstrated that the low MW inhibitor of SPHK1, SKI-5C, inhibits the development and vascularization of endometriotic lesions. Of interest, humanized monoclonal antibodies against S1P as well as SPHK2 inhibitors are already under clinical evaluation for the therapy of different cancer types and age-related macular degeneration (Britten et al., 2017; Pal et al., 2017; Volz & Pauly, 2015). Our novel findings now indicate that they may be also promising candidates for the future treatment of endometriosis, if they are proven to be safe and to exhibit a tolerable range of side effects.

ACKNOWLEDGEMENTS

We are grateful for the technical assistance of Janine Becker, Caroline Bickelmann, Sandra Hans and Ruth M. Nickels (Institute for Clinical & Experimental Surgery, Saarland University, Homburg/Saar, Germany). This work was supported by the research programme of Saarland University (61-cl/Anschub 2015).

AUTHOR CONTRIBUTIONS

J.R.-A., M.D.M. and M.W.L. participated in research design. J.R.-A. and A.C. conducted the experiments. J.R.-A. and A.C. performed data analysis. J.R.-A. and M.W.L. drafted the manuscript. J.R.-A., A.C., M.D.M. and M.W.L. critically revised the manuscript and gave approval to the final manuscript version.

CONFLICTS OF INTEREST

The authors declare no conflicts of interest.

DECLARATION OF TRANSPARENCY AND SCIENTIFIC RIGOUR

This Declaration acknowledges that this paper adheres to the principles for transparent reporting and scientific rigour of preclinical research as stated in the *BJP* guidelines for Design and Analysis, Immunoblotting and Immunochemistry and Animal Experimentation, and as recommended by funding agencies, publishers and other organisations engaged with supporting research.

DATA AVAILABILITY STATEMENT

The data that support the findings of this study are available from the corresponding author upon reasonable request. Some data may not be made available because of privacy or ethical restrictions.

ORCID

Matthias W. Laschke https://orcid.org/0000-0002-7847-8456

REFERENCES

Ader, I., Gstalder, C., Bouquerel, P., Golzio, M., Andrieu, G., Zalvidea, S., Richard, S., Sabbadini, R. A., Malavaud, B., & Cuvillier, O. (2015). Neutralizing S1P inhibits intratumoral hypoxia, induces vascular remodelling and sensitizes to chemotherapy in prostate cancer. *Oncotarget*, *6*(15), 13803–13821. https://doi.org/10.18632/oncotarget.3144

Ader, I., Malavaud, B., & Cuvillier, O. (2009). When the sphingosine kinase 1/sphingosine 1-phosphate pathway meets hypoxia signaling: New targets for cancer therapy. *Cancer Research*, *69*(9), 3723–3726. https://doi.org/10.1158/0008-5472

Alexander, S. P. H., Christopoulos, A., Davenport, A. P., Kelly, E., Mathie, A., Peters, J. A., Veale, E. L., Armstrong, J. F., Faccenda, E., Harding, S. D., & Pawson, A. J. (2019). The Concise Guide to

PHARMACOLOGY 2019/20: G protein-coupled receptors. *British Journal of Pharmacology*, *176*(S1), S21–S141. https://doi.org/10.1111/bph.14748

Alexander, S. P. H., Cidlowski, J. A., Kelly, E., Mathie, A., Peters, J. A., Veale, E. L., Armstrong, J. F., Faccenda, E., Harding, S. D., Pawson, A. J., & Sharman, J. L. (2019). The Concise Guide to PHARMACOLOGY 2019/20: Nuclear hormone receptors. *British Journal of Pharmacology*, *176*(S1), S229–S246. https://doi.org/10.1111/bph.14750

Alexander, S. P. H., Fabbro, D., Kelly, E., Mathie, A., Peters, J. A., Veale, E. L., Armstrong, J. F., Faccenda, E., Harding, S. D., Pawson, A. J., & Sharman, J. L. (2019a). The Concise Guide to PHARMACOLOGY 2019/20: Catalytic receptors. *British Journal of Pharmacology*, *176*(S1), S247–S296.

Alexander, S. P. H., Fabbro, D., Kelly, E., Mathie, A., Peters, J. A., Veale, E. L., Armstrong, J. F., Faccenda, E., Harding, S. D., Pawson, A. J., & Sharman, J. L. (2019b). The Concise Guide to PHARMACOLOGY 2019/20: Enzymes. *British Journal of Pharmacology*, *176*(S1), S297–S396. https://doi.org/10.1111/bph.14752

Alexander, S. P. H., Kelly, E., Mathie, A., Peters, J. A., Veale, E. L., Armstrong, J. F., Faccenda, E., Harding, S. D., Pawson, A. J., Sharman, J. L., & Southan, C. (2019a). The Concise Guide to PHARMACOLOGY 2019/20: Introduction and other protein targets. *British Journal of Pharmacology*, *176*(S1), S1–S20. https://doi.org/10.1111/bph.14747

Alexander, S. P. H., Kelly, E., Mathie, A., Peters, J. A., Veale, E. L., Armstrong, J. F., Faccenda, E., Harding, S. D., Pawson, A. J., Sharman, J. L., & Southan, C. (2019b). The Concise Guide to PHARMACOLOGY 2019/20: Transporters. *British Journal of Pharmacology*, *176*(S1), S397–S493. https://doi.org/10.1111/bph.14753

Alexander, S. P. H., Roberts, R. E., Broughton, B. R. S., Sobey, C. G., George, C. H., Stanford, S. C., Cirino, G., Docherty, J. R., Giembycz, M. A., Hoyer, D., & Insel, P. A. (2018). Goals and practicalities of immunoblotting and immunohistochemistry: A guide for submission to the British Journal of pharmacology. *British Journal of Pharmacology*, *175*(3), 407–411. https://doi.org/10.1111/bph.14112

Attar, E., Tokunaga, H., Imir, G., Yilmaz, M. B., Redwine, D., Putman, M., Gurates, B., Attar, R., Yaegashi, N., Hales, D. B., & Bulun, S. E. (2009). Prostaglandin E2 via steroidogenic factor-1 coordinately regulates transcription of steroidogenic genes necessary for estrogen synthesis in endometriosis. *The Journal of Clinical Endocrinology and Metabolism*, *94*(2), 623–631. https://doi.org/10.1210/jc.2008-1180

Becker, C. M., Rohwer, N., Funakoshi, T., Cramer, T., Bernhardt, W., Birsner, A., Folkman, J., & D'Amato, R. J. (2008). 2-methoxyestradiol inhibits hypoxia-inducible factor-1{alpha} and suppresses growth of lesions in a mouse model of endometriosis. *The American Journal of Pathology*, *172*(2), 534–544. https://doi.org/10.2353/ajpath.2008.061244

Bedaiwy, M. A., Alfaraj, S., Yong, P., & Casper, R. (2017). New developments in the medical treatment of endometriosis. *Fertility and Sterility*, *107*(3), 555–565. https://doi.org/10.1016/j.fertnstert.2016.12.025

Bergqvist, A., Bruse, C., Carlberg, M., & Carlström, K. (2001). Interleukin 1beta, interleukin-6, and tumor necrosis factor-alpha in endometriotic tissue and in endometrium. *Fertility and Sterility*, *75*(3), 489–495. https://doi.org/10.1016/s0015-0282(00)01752-0

Blaho, V. A., & Hla, T. (2014). An update on the biology of sphingosine 1-phosphate receptors. *Journal of Lipid Research*, *55*(8), 1596–1608. https://doi.org/10.1194/jlr.R046300

Britten, C. D., Garrett-Mayer, E., Chin, S. H., Shirai, K., Ogretmen, B., Bentz, T. A., Brisendine, A., Anderton, K., Cusack, S. L., Maines, L. W., Zhuang, Y., Smith, C. D., & Thomas, M. B. (2017). A phase I study of ABC294640, a first-in-class sphingosine Kinase-2 inhibitor, in patients with advanced solid tumors. *Clinical Cancer Research*, *23*(16), 4642–4650. https://doi.org/10.1158/1078-0432.CCR-16-2363

Brünnert, D., Sztachelska, M., Bornkessel, F., Treder, N., Wolczynski, S., Goyal, P., & Zygmunt, M. (2014). Lysophosphatidic acid and sphingosine 1-phosphate metabolic pathways and their receptors are differentially regulated during decidualization of human endometrial stromal cells. *Molecular Human Reproduction*, *20*(10), 1016–1025. https://doi.org/10.1093/molehr/gau051

Burney, R. O., & Giudice, L. C. (2012). Pathogenesis and pathophysiology of endometriosis. *Fertility and Sterility*, *98*(3), 511–519. https://doi.org/10.1016/j.fertnstert.2012.06.029

Burns, K. A., Rodriguez, K. F., Hewitt, S. C., Janardhan, K. S., Young, S. L., & Korach, K. S. (2012). Role of estrogen receptor signaling required for endometriosis-like lesion establishment in a mouse model. *Endocrinology*, *153*(8), 3960–3971. https://doi.org/10.1016/j.fertnstert.2012.06.029

Curtis, M. J., Alexander, S., Cirino, G., Docherty, J. R., George, C. H., Giembycz, M. A., Hoyer, D., Insel, P. A., Izzo, A. A., Ji, Y., MacEwan, D. J., Sobey, C. G., Stanford, S. C., Teixeira, M. M., Wonnacott, S., & Ahluwalia, A. (2018). Experimental design and analysis and their reporting II: Updated and simplified guidance for authors and peer reviewers. *British Journal of Pharmacology*, *175*(7), 987–993. https://doi.org/10.1111/bph.14153

Dai, L., Liu, Y., Xie, L., Wu, X., Qiu, L., & Di, W. (2017). Sphingosine kinase 1/sphingosine-1-phosphate (S1P)/S1P receptor axis is involved in ovarian cancer angiogenesis. *Oncotarget*, *8*(43), 74947–74961. https://doi.org/10.18632/oncotarget.20471

Datta, A., Loo, S. Y., Huang, B., Wong, L., Tan, S. S., Tan, T. Z., Lee, S. C., Thiery, J. P., Lim, Y. C., Yong, W. P., & Lam, Y. (2014). SPHK1 regulates proliferation and survival responses in triple-negative breast cancer. *Oncotarget*, *5*(15), 5920–5933. https://doi.org/10.18632/oncotarget.1874

Furuya, H., Tamashiro, P. M., Shimizu, Y., Iino, K., Peres, R., Chen, R., Sun, Y., Hannun, Y. A., Obeid, L. M., & Kawamori, T. (2017). Sphingosine kinase 1 expression in peritoneal macrophages is required for colon carcinogenesis. *Carcinogenesis*, *38*, 1218–1227. https://doi.org/10.1093/carcin/bgx104

Gaengel, K., Niaudet, C., Hagikura, K., Laviña, B., Muhl, L., Hofmann, J. J., Ebarasi, L., Nyström, S., Rymo, S., Chen, L. L., Pang, M. F., Jin, Y., Raschperger, E., Roswall, P., Schulte, D., Benedito, R., Larsson, J., Hellström, M., Fuxe, J., … Betsholtz, C. (2012). The sphingosine-1-phosphate receptor S1PR1 restricts sprouting angiogenesis by regulating the interplay between VE-cadherin and VEGFR2. *Developmental Cell*, *23*(3), 587–599. https://doi.org/10.1016/j.devcel.2012.08.005

González-Ramos, R., Van Langendonckt, A., Defrère, S., Lousse, J. C., Colette, S., Devoto, L., & Donnez, J. (2010). Involvement of the nuclear factor-κB pathway in the pathogenesis of endometriosis. *Fertility and Sterility*, *94*(6), 1985–1994. https://doi.org/10.1016/j.fertnstert.2010.01.013

González-Ramos, R., Van Langendonckt, A., Defrère, S., Lousse, J. C., Mettlen, M., Guillet, A., & Donnez, J. (2008). Agents blocking the nuclear factor-kappaB pathway are effective inhibitors of endometriosis in an in vivo experimental model. *Gynecologic and Obstetric Investigation*, *65*(3), 174–186. https://doi.org/10.1159/000111148

Greaves, E., Cousins, F. L., Murray, A., Esnal-Zufiaurre, A., Fassbender, A., Horne, A. W., & Saunders, P. T. (2014). A novel mouse model of endometriosis mimics human phenotype and reveals insights into the inflammatory contribution of shed endometrium. *The American Journal of Pathology*, *184*(7), 1930–1939. https://doi.org/10.1016/j.ajpath.2014.03.011

Greaves, E., Horne, A. W., Jerina, H., Mikolajczak, M., Hilferty, L., Mitchell, R., Fleetwood-Walker, S. M., & Saunders, P. T. (2017). EP(2) receptor antagonism reduces peripheral and central hyperalgesia in a preclinical mouse model of endometriosis. *Scientific Reports*, *7*, 44169–44180. https://doi.org/10.1038/srep44169

Groothuis, P. G., Nap, A. W., Winterhager, E., & Grümmer, R. (2005). Vascular development in endometriosis. *Angiogenesis*, *8*(2), 147–156. https://doi.org/10.1007/s10456-005-9005-x

Hisano, Y., & Hla, T. (2019). Bioactive lysolipids in cancer and angiogenesis. *Pharmacology & Therapeutics*, *193*, 91–98. https://doi.org/10.1016/j.pharmthera.2018.07.006

Hla, T., Lee, M. J., Ancellin, N., Paik, J. H., & Kluk, M. J. (2001). Lysophospholipids--receptor revelations. *Science*, *294*(5548), 1875–1878. https://doi.org/10.1126/science.1065323

Kiani, K., Rudzitis-Auth, J., Scheuer, C., Movahedin, M., Sadati Lamardi, S. N., Malekafzali Ardakani, H., Becker, V., Moini, A., Aflatoonian, R., Ostad, S. N., Menger, M. D., & Laschke, M. W. (2019). Calligonum comosum (Escanbil) extract exerts anti-angiogenic, anti-proliferative and anti-inflammatory effects on endometriotic lesions. *Journal of Ethnopharmacology*, *239*, 111918. https://doi.org/10.1016/j.jep.2019.111918

Kunkel, G. T., Maceyka, M., Milstien, S., & Spiegel, S. (2013). Targeting the sphingosine-1-phosphate axis in cancer, inflammation and beyond. *Nature Reviews. Drug Discovery*, *12*(9), 688–702. https://doi.org/10.1038/nrd4099

Laschke, M. W., Giebels, C., Nickels, R. M., Scheuer, C., & Menger, M. D. (2011). Endothelial progenitor cells contribute to the vascularization of endometriotic lesions. *The American Journal of Pathology*, *178*(1), 442–450. https://doi.org/10.1016/j.ajpath.2010.11.037

Laschke, M. W., Körbel, C., Rudzitis-Auth, J., Gashaw, I., Reinhardt, M., Hauff, P., Zollner, T. M., & Menger, M. D. (2010). High-resolution ultrasound imaging: A novel technique for the noninvasive in vivo analysis of endometriotic lesion and cyst formation in small animal models. *The American Journal of Pathology*, *176*(2), 585–593. https://doi.org/10.2353/ajpath.2010.090617

Laschke, M. W., & Menger, M. D. (2018). Basic mechanisms of vascularization in endometriosis and their clinical implications. *Human Reproduction Update*, *24*(2), 207–224. https://doi.org/10.1093/humupd/dmy001

Laschke, M. W., Vollmar, B., & Menger, M. D. (2011). The dorsal skinfold chamber: Window into the dynamic interaction of biomaterials with their surrounding host tissue. *European Cells & Materials*, *22*, 147–164. https://doi.org/10.22203/ecm.v022a12

Laschke, M. W., Vorsterman van Oijen, A. E., Scheuer, C., & Menger, M. D. (2011). In vitro and in vivo evaluation of the anti-angiogenic actions of 4-hydroxybenzyl alcohol. *British Journal of Pharmacology*, *163*(4), 835–844. https://doi.org/10.1111/j.1476-5381.2011.01292.x

Lee, M. J., Thangada, S., Claffey, K. P., Ancellin, N., Liu, C. H., Kluk, M., Volpi, M., Sha'afi, R. I., & Hla, T. (1999). Vascular endothelial cell adherens junction assembly and morphogenesis induced by sphingosine-1-phosphate. *Cell*, *99*(3), 301–312. https://doi.org/10.1016/s0092-8674(00)81661-x

Li, P. H., Wu, J. X., Zheng, J. N., & Pei, D. S. (2014). A sphingosine kinase-1 inhibitor, SKI-II, induces growth inhibition and apoptosis in human gastric cancer cells. *Asian Pacific Journal of Cancer Prevention*, *15*(23), 10381–20385. https://doi.org/10.7314/apjcp.2014.15.23.10381

Li, S., Zhou, Y., Zheng, X., Wu, X., Liang, Y., Wang, S., & Zhang, Y. (2016). Sphk1 promotes breast epithelial cell proliferation via NF-κB-p65-mediated cyclin D1 expression. *Oncotarget*, *7*(49), 80579–80585. https://doi.org/10.18632/oncotarget.13013

Lilley, E., Stanford, S. C., Kendall, D. E., Alexander, S. P., Cirino, G., Docherty, J. R., George, C. H., Insel, P. A., Izzo, A. A., Ji, Y., Panettieri, R. A., Sobey, C. G., Stefanska, B., Stephens, G., Teixeira, M., & Ahluwalia, A. (2020). ARRIVE 2.0 and the British Journal of Pharmacology: Updated guidance for 2020. *British Journal of Pharmacology*, *177*(16), 3611–3616. https://doi.org/10.1111/bph.15178

Liu, H., Chakravarty, D., Maceyka, M., Milstien, S., & Spiegel, S. (2002). Sphingosine kinases: A novel family of lipid kinases. *Progress in Nucleic Acid Research and Molecular Biology*, *71*, 493–511. https://doi.org/10.1016/s0079-6603(02)71049-0

Liu, Y., Wada, R., Yamashita, T., Mi, Y., Deng, C. X., Hobson, J. P., Rosenfeldt, H. M., Nava, V. E., Chae, S. S., Lee, M. J., Liu, C. H., Hla, T., Spiegel, S., & Proia, R. L. (2000). Edg-1, the G protein-coupled receptor for sphingosine-1-phosphate, is essential for vascular maturation. *The Journal of Clinical Investigation*, *106*(8), 951–961. https://doi.org/10.1172/JCI10905

Mathews, T. P., Kennedy, A. J., Kharel, Y., Kennedy, P. C., Nicoara, O., Sunkara, M., Morris, A. J., Wamhoff, B. R., Lynch, K. R., & Macdonald, T. L. (2010). Discovery, biological evaluation, and structure-activity relationship of amidine based sphingosine kinase inhibitors. *Journal of Medicinal Chemistry*, *53*(7), 2766–2778. https://doi.org/10.1021/jm901860h

Mizugishi, K., Li, C., Olivera, A., Bielawski, J., Bielawska, A., Deng, C. X., & Proia, R. L. (2007). Maternal disturbance in activated sphingolipid metabolism causes pregnancy loss in mice. *The Journal of Clinical Investigation*, *117*(10), 2993–3006. https://doi.org/10.1172/JCI30674

Mizugishi, K., Yamashita, T., Olivera, A., Miller, G. F., Spiegel, S., & Proia, R. L. (2005). Essential role for sphingosine kinases in neural and vascular development. *Molecular and Cellular Biology*, *25*(24), 11113–11121. https://doi.org/10.1128/MCB.25.24.11113-11121.2005

Nagahashi, M., Kim, E. Y., Yamada, A., Ramachandran, S., Allegood, J. C., Hait, N. C., Maceyka, M., Milstien, S., Takabe, K., & Spiegel, S. (2013). Spns2, a transporter of phosphorylated sphingoid bases, regulates their blood and lymph levels, and the lymphatic network. *The FASEB Journal*, *27*(3), 1001–1011. https://doi.org/10.1096/fj.12-219618

Nasu, K., Nishida, M., Ueda, T., Yuge, A., Takai, N., & Narahara, H. (2007). Application of the nuclear factor-kappaB inhibitor BAY 11-7085 for the treatment of endometriosis: An in vitro study. *American Journal of Physiology. Endocrinology and Metabolism*, *293*(1), E16–E23. https://doi.org/10.1152/ajpendo.00135.2006

O'Brien, N., Jones, S. T., Williams, D. G., Cunningham, H. B., Moreno, K., Visentin, B., Gentile, A., Vekich, J., Shestowsky, W., Hiraiwa, M., & Matteo, R. (2009). Production and characterization of monoclonal anti-sphingosine-1-phosphate antibodies. *Journal of Lipid Research*, *50*(11), 2245–2257. https://doi.org/10.1194/jlr.M900048-JLR200

Olivera, A., Rosenfeldt, H. M., Bektas, M., Wang, F., Ishii, I., Chun, J., Milstien, S., & Spiegel, S. (2003). Sphingosine kinase type 1 induces G12/13-mediated stress fiber formation, yet promotes growth and survival independent of G protein-coupled receptors. *The Journal of Biological Chemistry*, *278*(47), 46452–44660. https://doi.org/10.1074/jbc.M308749200

Pal, S. K., Drabkin, H. A., Reeves, J. A., Hainsworth, J. D., Hazel, S. E., Paggiarino, D. A., Wojciak, J., Woodnutt, G., & Bhatt, R. S. (2017). A phase 2 study of the sphingosine-1-phosphate antibody sonepcizumab in patients with metastatic renal cell carcinoma. *Cancer*, *123*(4), 576–582. https://doi.org/10.1002/cncr.30393

Percie du Sert, N., Hurst, V., Ahluwalia, A., Alam, S., Avey, M. T., Baker, M., Browne, W. J., Clark, A., Cuthill, I. C., Dirnagl, U., Emerson, M., Garner, P., Holgate, S. T., Howells, D. W., Karp, N. A., Lazic, S. E., Lidster, K., MacCallum, C. J., Macleod, M., … Würbel, H. (2020). The ARRIVE guidelines 2.0: updated guidelines for reporting animal research. *PLoS Biology*, *18*(7), e3000410. https://doi.org/10.1371/journal.pbio.3000410

Peterse, D., Clercq, K., Goossens, C., Binda, M. M., Dorien, F. O., Saunders, P., Vriens, J., Fassbender, A., & D'Hooghe, T. M. (2018). Optimization of endometrial Decidualization in the menstruating mouse model for preclinical endometriosis research. *Reproductive Sciences*, *25*, 1577–1588. https://doi.org/10.1177/1933719118756744

Ramathal, C. Y., Bagchi, I. C., Taylor, R. N., & Bagchi, M. K. (2010). Endometrial decidualization: Of mice and men. *Seminars in*

Reproductive Medicine, *28*(1), 17–26. https://doi.org/10.1055/s-0029-1242989

Reynolds, L. P., Grazul-Bilska, A. T., & Redmer, D. A. (2002). Angiogenesis in the female reproductive organs: Pathological implications. *International Journal of Experimental Pathology*, *83*(4), 151–163. https://doi.org/10.1046/j.1365-2613.2002.00277.x

Rocha, A. L., Reis, F. M., & Taylor, R. N. (2013). Angiogenesis and endometriosis. *Obstetrics and Gynecology International*, *2013*, 859619–8. https://doi.org/10.1155/2013/859619

Rudzitis-Auth, J., Fuß, S. A., Becker, V., Menger, M. D., & Laschke, M. W. (2020). Inhibition of erythropoietin-producing hepatoma receptor B4 (EphB4) signalling suppresses the vascularisation and growth of endometriotic lesions. *British Journal of Pharmacology*, *177*(14), 3225–3239. https://doi.org/10.1111/bph.15044

Rudzitis-Auth, J., Nickels, R. M., Menger, M. D., & Laschke, M. W. (2018). Inhibition of Cyclooxygenase-2 suppresses the recruitment of endothelial progenitor cells in the microvasculature of Endometriotic lesions. *The American Journal of Pathology*, *188*(2), 450–460. https://doi.org/10.1016/j.ajpath.2017.10.013

Rumzhum, N. N., Rahman, M. M., Oliver, B. G., & Ammit, A. J. (2016). Effect of sphingosine 1-phosphate on Cyclo-Oxygenase-2 expression, prostaglandin E2 secretion, and β2-adrenergic receptor desensitization. *American Journal of Respiratory Cell and Molecular Biology*, *54*(1), 128–135. https://doi.org/10.1165/rcmb.2014-0443OC

Sampson, J. A. (1927). Peritoneal endometriosis due to menstrual dissemination of endometrial tissues into the peritoneal cavity. *American Journal of Obstetrics and Gynecology*, *14*(4), 422–469. https://doi.org/10.1016/S0002-9378(15)30003-X

Sanchez, T., & Hla, T. (2004). Structural and functional characteristics of S1P receptors. *Journal of Cellular Biochemistry*, *92*(5), 913–922. https://doi.org/10.1002/jcb.20127

Santulli, P., Marcellin, L., Noël, J. C., Borghese, B., Fayt, I., Vaiman, D., Chapron, C., & Méhats, C. (2012). Sphingosine pathway deregulation in endometriotic tissues. *Fertility and Sterility*, *97*(4), 904–911. https://doi.org/10.1016/j.fertnstert.2011.12.051

Soliman, A. M., Yang, H., Du, E. X., Kelley, C., & Winkel, C. (2016). The direct and indirect costs associated with endometriosis: A systematic literature review. *Human Reproduction*, *31*(4), 712–722. https://doi.org/10.1093/humrep/dev335

Sukocheva, O., Wadham, C., Gamble, J., & Xia, P. (2015). Sphingosine-1-phosphate receptor 1 transmits estrogens' effects in endothelial cells. *Steroids*, *104*, 237–245. https://doi.org/10.1016/j.steroids.2015.10.009

Visentin, B., Vekich, J. A., Sibbald, B. J., Cavalli, A. L., Moreno, K. M., Matteo, R. G., Garland, W. A., Lu, Y., Yu, S., Hall, H. S., Kundra, V., Mills, G. B., & Sabbadini, R. A. (2006). Validation of an anti-sphingosine-1-phosphate antibody as a potential therapeutic in reducing growth, invasion, and angiogenesis in multiple tumor lineages. *Cancer Cell*, *9*(3), 225–238. https://doi.org/10.1016/j.ccr.2006.02.023

Volz, C., & Pauly, D. (2015). Antibody therapies and their challenges in the treatment of age-related macular degeneration. *European Journal of Pharmaceutics and Biopharmaceutics*, *95*, 158–172. https://doi.org/10.1016/j.ejpb.2015.02.020

von Otte, S., Paletta, J. R., Becker, S., König, S., Fobker, M., Greb, R. R., Kiesel, L., Assmann, G., Diedrich, K., & Nofer, J. R. (2006). Follicular fluid high density lipoprotein-associated sphingosine 1-phosphate is a novel mediator of ovarian angiogenesis. *The Journal of Biological Chemistry*, *281*(9), 5398–5405. https://doi.org/10.1074/jbc.M508759200

Yoshino, O., Yamada-Nomoto, K., Kano, K., Ono, Y., Kobayashi, M., Ito, M., Yoneda, S., Nakashima, A., Shima, T., Onda, T., Osuga, Y., Aoki, J., & Saito, S. (2019). Sphingosine 1 phosphate (S1P) increased IL-6 expression and cell growth in Endometriotic cells. *Reproductive Sciences*, *26*(11), 1460–1467. https://doi.org/10.1177/1933719119828112

Young, N., & Van Brocklyn, J. R. (2006). Signal transduction of sphingosine-1-phosphate G protein-coupled receptors. *ScientificWorldJournal*, *6*, 946–966. https://doi.org/10.1100/tsw.2006.182

Zhao, Y., Gong, P., Chen, Y., Nwachukwu, J. C., Srinivasan, S., Ko, C., Bagchi, M. K., Taylor, R. N., Korach, K. S., Nettles, K. W., Katzenellenbogen, J. A., & Katzenellenbogen, B. S. (2015). Dual suppression of estrogenic and inflammatory activities for targeting of endometriosis. *Science Translational Medicine*, *7*, 271ra9. https://doi.org/10.1126/scitranslmed.3010626

How to cite this article: Rudzitis-Auth, J., Christoffel, A., Menger, M. D., & Laschke, M. W. (2021). Targeting sphingosine kinase-1 with the low MW inhibitor SKI-5C suppresses the development of endometriotic lesions in mice. *British Journal of Pharmacology*, *178*(20), 4104–4118. https://doi.org/10.1111/bph.15601